Contents lists available at YXpublications

International Journal of Applied Mathematics in Control Engineering

Journal homepage: http://www.ijamce.com

Fixed-time Adaptive Neural Network Sliding Mode Control for Uncertain Nonlinear Systems and Application to Quadrotor UAVs Tracking Control

Wenbo Fei[a], Jin Tian[a], Xueli Wu[a,*]

[a] *Hebei University of Science and Technology, Shijiazhuang, Hebei, 050018, China*

ARTICLE INFO

Article history:
Received 2 March 2021
Accepted 3 May 2021
Available online 5 May 2021

Keywords:
Fixed-time control
Radial basis function neural networks
Dual-power approach rate
Non-singular fast terminal sliding mode
Quadrotor unmanned aerial vehicle

ABSTRACT

This paper uses a fixed-time radial basis function neural network adaptive law, non-singular fast terminal sliding mode(NFTSM) function, and fixed-time dual-power approach rate to solve the unknown nonlinear function, convergence speed, singularity problem, and robust performance in uncertain nonlinear systems. Using the scaling method proves that the system can reach a fixed-time convergence. Through the tracking control of the quadrotor unmanned aerial vehicle, it is proved that the algorithm can solve the complex nonlinear problem. Finally, a large number of numerical examples are used to verify the effectiveness of the content presented in this paper.

1. Introduction

The development of nonlinear systems and linear systems is almost parallel (Khalil, 2020), but in fact, almost all systems have different uncertainties and nonlinearities, so nonlinear system control problems have always been one of the hot spots in the academic engineering field. Many theoretical methods in modern control theory use linear systems as their basic research objects. But in the field of actual engineering, we try our best to get the precise mathematical model of the system, but due to uncertain interference and other factors, we have to solve a series of nonlinear problems. Linear models cannot be applied at all in some controlled objects, such as aircraft tracking control (Yao et al., 2020) , robotic arm systems (Li et al., 2019), multi-agent formation (Wang et al., 2020b), etc. we require extremely high control accuracy, so for nonlinear system models, a nonlinear control strategy must be adopted to meet the needs.

The control of nonlinear systems can be divided into two aspects: system analysis and controller system design. In the former, the phase plane method and description function method are applied to the research object to realize the absolute stability of the nonlinear system. The latter is to design control laws for nonlinear systems to achieve control tracking, such as adaptive control (Zhihua et al., 2006), robust control (Krishnamurthy et al., 2009) , differential algebra (Franco et al., 2020), backstepping (Bi and Shi, 2017),NNs (Li et al., 2015),sliding mode control (Fujimoto et al., 2021) and fuzzy control (Wang et al., 2019), etc. As we all know, scholars have provided a large number of effective strategies for nonlinear system control, and provided a large amount of theoretical foundation for practical engineering applications. In (Zeng Lian and Svoboda, 2006), scholars proposed a sliding mode fuzzy NN learning control strategy based on disturbance observer, which can maintain stable performance in the presence of disturbance. In (Chen and Chen, 2007), this paper proposes a linear LTR robust observer for the Lipchitz nonlinear system, which has good reliability in the face of large interference. In (Yin et al., 2010), scholars designed a new iterative learning control scheme for nonlinear systems with parameter uncertainties, and experiments proved the effectiveness of iterative learning strategies with high-order internal models. In (Guifang and Chen, 2018), a display controller was established in the gradient direction to deal with the random nonlinear system with matching conditions, so that the closed-loop system response was globally restricted in probability, and an example was given to verify the validity. In (Li et al., 2021), to solve the influence of event triggering, the author proposes an adaptive finite-time event triggering controller to solve the problems in uncertain nonlinear systems. In (Zhang and Wang, 2021), The author uses observers and NNs to solve the problems of unmeasurable states and unknown nonlinearities, and achieves fixed time control. Obviously, the finite time control strategy has been widely recognized by scholars and a lot of research has been done.

* Corresponding author.
E-mail addresses: wuxueli@hebust.edu.cn (X. Wu)

Due to the complexity and variability of nonlinear systems, scholars have carried out targeted research on nonlinear systems under different conditions and proposed effective control strategies. This paper proposes a non-singular fast terminal fixed-time dual-power sliding mode control based on an adaptive NN for nonlinear systems with uncertain disturbances. At the same time, a reliable fixed-time tracking control strategy is provided for the under-driving uncertain nonlinear system of the quadrotor.

Because the quadrotor system itself is an under-driving system with four inputs and six outputs, plus the uncertainty of the actual working environment, the quad-rotor system is a rather complex nonlinear system. At the same time, because quadrotor UAVs have a large number of applications in many fields, such as aerial photography (Huang et al., 2016), plant protection drones (Ma et al., 2019), reconnaissance (Mintchev and Floreano, 2016), etc. The research on quadrotor UAVs is of great significance and there are already a large number of research results. In (Kim and Ahn, 2019), scholars provided an advanced attitude tracking controller for quadrotor UAVs that combines an automatic tuner and a disturbance observer. The Lyapunov stability was used to prove the offset-free convergence and performance recovery characteristics. In (Santoso et al., 2020), in order to adapt to the uncertain interference faced by the quadcopter, hybrid feedback and feedforward autopilot is proposed, which uses nonlinear model prediction technology to solve the problem of accurate tracking. As we all know, NNs have superior performance in dealing with nonlinear system problems. In (Wu et al., 2009), the author applied an adaptive recurrent NN to study a kind of nonlinear dynamic system with real-time delay for identification and control.In(Salt et al., 2020), The author uses a fast-responding spiked NN structure to provide reliable data support for the quadrotor dynamic vision sensor. Obviously, there have been a lot of academic achievements in the control research of quadrotor UAVs. However, due to practical needs, the problem of finite time stability has become a hot research topic today (Wu et al., 2021, Gao and Guo, 2020, Yang and Niu, 2020). In the control research of quadrotor UAVs, in order to enhance the control performance, the author solved the problem of quality change in the operation of the aircraft (Wang et al., 2020a), and some scholars proposed fixed-time control to improve the stability performance (Zhang et al., 2020a). In the above research results, it is inevitable that some scholars have overlooked the convergence speed, singularity, robust performance, and practical fixed-time convergence problems. As we all know, these problems have a great impact on the control and work efficiency of quadrotor UAVs.

In the first section of the article, the nonlinear system problems and basic lemmas are given. In the second section, a fixed-time controller is designed and the necessary proofs are made. In the third section, the quadrotor UAV controller. Finally, the algorithm is verified by numerical examples. The main contributions of this paper can be as follows:

The design of fixed-time dual-power sliding mode control law based on NFTSM function can effectively solve the problems of chattering and slow convergence in traditional sliding mode control so that the system can be stable in finite time. The algorithm solved the possible singular problems.

Design a fixed-time NN adaptive law, which can approximate an uncertain nonlinear system in a finite time without considering the ideal weight and the initial value of the weight.

The algorithm can ensure stability under large interference conditions. Compare the algorithm proposed in this paper with the paper (Alqaisi et al., 2020) in terms of robust performance.

2. Problem formulation and preliminary

Consider the following second-order uncertain nonlinear system:

$$\begin{aligned} x_1 &= \dot{x}_2 \\ x_2 &= \Lambda u + f(x) + dt(x,t) \end{aligned} \tag{1}$$

Where $x \in R^n$ is the state of the system, $f(x)$ is the known vector field, $u \in R$ is the control input, Λ is a real number and $dt \in R$ is the uncertain disturbance. The purpose is to elicit the tracking control research of the quadrotor UAVs through the above-mentioned nonlinear system.

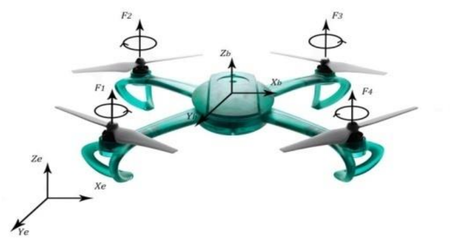

Fig. 1. Schematic of the quadrotor UAV system.

Taking into account the quadrotor UAV system shown in Fig.1(Song et al., 2019),the body coordinate system and the ground coordinate system are selected, and the mathematical model of the quadrotor system is obtained according to the coordinate system and system dynamics model, using Newton's Euler equations. The attitude angle is expressed as yaw angle ψ , pitch angle θ, and roll angle ϕ. Assuming that the quadcopter is a rigid body, its dynamic model can be expressed as:

Position dynamic equation:

$$\ddot{x} = Au_x(t) + f_x(\cdot) + d_a \tag{2}$$

Attitude dynamic equation:

$$\ddot{p} = Bu_p(t) + f_p(\cdot) + d_b \tag{3}$$

$$\begin{aligned} P_x &= F_{at}(\sin\phi\sin\psi + \cos\phi\sin\theta\cos\psi) \\ P_y &= F_{at}\left(\sin\theta\sin\psi\cos\phi - \cos\psi\sin\phi\right) \\ P_z &= F_{at}(\cos\phi\cos\theta) \end{aligned} \tag{4}$$

$$u_1 = F_{at}, u_\phi = \tau_{a\phi}, u_\theta = \tau_{a\theta}, u_\psi = \tau_{a\psi} \tag{5}$$

$$\begin{aligned} a &= \frac{I_y - I_z}{I_x}\dot{\theta}\dot{\psi} - \frac{I_r}{I_x}\dot{\theta}\varpi - \frac{\xi_\phi}{I_x} \\ b &= \frac{I_z - I_x}{I_y}\dot{\phi}\dot{\psi} - \frac{I_r}{I_y}\dot{\phi}\varpi - \frac{\xi_\theta}{I_y} \\ c &= -\frac{\xi_\psi}{I_z}, d = \frac{1}{m} \end{aligned} \tag{6}$$

Where $A = diag(d,d,d)$ $B = diag(\frac{1}{I_x},\frac{1}{I_y},\frac{1}{I_z})$,

$$u_x(t) = \left[P_x, P_y, P_z\right]^T \; u_p(t) = \left[u_\phi, u_\theta, u_\psi\right]^T \in R^3$$

$$f_1(\cdot) = \left[-\xi_x d\dot{x}, -\xi_y d\dot{y}, -\xi_z d\dot{z} - g\right]^T \in R^3,\; f_2(\cdot) = \left[a,b,c\right]^T \in R^3,$$

$$A, B \in R^{3\times3}, u_x(t), u_P(t) \in R^3,$$

m is the mass of the quadrotor UAVs, $I = diag(I_x, I_y, I_z)$ is the moment of inertia of the three coordinate axes in the body coordinate system, g is the selected acceleration of gravity, $\xi = \left[\xi_x, \xi_y, \xi_z, \xi_\phi, \xi_\theta, \xi_\psi\right]^T$ is the air drag coefficient, I_r is the rotor inertia, and $\overline{w} = w_4 + w_3 - w_2 - w_1$ is the total remaining rotor Angle.

$d_a(\cdot) = \left[d_x, d_y, d_z\right]^T \in R^3, d_b(\cdot) = \left[d_\phi, d_\theta, d_\psi\right]^T \in R^3$ are uncertain disturbances in the position and attitude system. F_{at} represents the combined force of the control thrust in the three directions, and $\tau_{a\phi}, \tau_{a\theta}, \tau_{a\psi}$ is the torque generated by the rotation.

Remark 1. Converting the quadrotor model (2)(3) to the above-mentioned form (1) is convenient for the development of problem research and unnecessary and repetitive proofs, and can convert the theorems obtained in uncertain nonlinear systems to quadrotor UAVs under system control.

Lemma 1 (Chen et al., 2019, Jiang et al., 2016)**.** Suppose the system exists a Lyapunov function $V(\cdot): R^n \to R_+ \cup \{0\}$, where scalars $\alpha, \beta, p, q, \tau \in R^+$ are positive real numbers with $0 < p\tau < 1, q\tau > 1$ and $0 < \delta < \infty$. Such that

$$V(x) = 0 \Leftrightarrow x = 0 \tag{7}$$

$$\dot{V}(x) \le -(\alpha V(x)^p)^\tau - (\beta V(x)^q)^\tau + \delta \tag{8}$$

Then the origin $x = 0$ of system $\dot{x} = f(t,x), x(0) = x_0$ is practically fixed-time stable. The residual set of the system solution can be given by

$$\left\{ \lim_{t\to T} x \,\middle|\, V(x) \le \min\left\{ \alpha^{\frac{-1}{p}} (\frac{\delta}{1-\partial^\tau})^{\frac{1}{p\tau}}, \beta^{\frac{-1}{p}} (\frac{\delta}{1-\partial^\tau})^{\frac{1}{q\tau}} \right\} \right\} \tag{9}$$

where scalar satisfies $0 < \partial < 1$,then the time is bounded as

$$T_{\max} = \frac{1}{2^{p\tau-1}\alpha(1-p\tau)} + \frac{1}{\beta(q\tau-1)} \tag{10}$$

Lemma 2 (Zhang et al., 2020b)**.** For any constant $a, b \in R$, $g > 1, h > 1$ and $\frac{1}{g} + \frac{1}{h} = 1$ the following Young's inequality holds:

$$ab \le \frac{1}{g}a^g + \frac{1}{h}b^h \tag{11}$$

Lemma 3 (Zhang et al., 2019)**.**For positive constant $\rho = \frac{1}{3}$, vector quantity $W^*, \hat{W}, \tilde{W} \in R^m$ and satisfy $\tilde{W} = \hat{W} - W^*$ .According to Young's inequality, the following inequality holds:

$$-\tilde{W}^T \hat{W}^\rho \le -\frac{1}{2}\tilde{W}^{\frac{\rho+1}{2}T}\tilde{W}^{\frac{\rho+1}{2}} + W^{*\frac{\rho+1}{2}T} W^{*\frac{\rho+1}{2}} \tag{12}$$

Where $\tilde{W} = \left[\tilde{x}_1, \tilde{x}_2, \tilde{x}_3 \cdots \tilde{x}_n\right]^T, \hat{W} = \left[\hat{x}_1, \hat{x}_2, \hat{x}_3 \cdots \hat{x}_n\right]^T$,

$W^* = \left[x_1^*, x_2^*, x_3^* \cdots x_n^*\right]^T, \hat{W}^\rho = \left[\hat{x}_1^\rho, \hat{x}_2^\rho, \hat{x}_3^\rho \cdots \hat{x}_n^\rho\right]^T$

$\tilde{W}, \hat{W}, W^*, \hat{W}^\rho \in R^n$.

Lemma 4 (Xiao et al., 2017)**.**For $h = \left[h_1, h_2, h_3 \cdots h_i\right]^T \in R^i$, and the constants $0 < n \le 1, m > 1$,then the following inequality hold:

$$(\sum_{j=1}^{i} |h_j|)^n \le \sum_{j=1}^{i} |h_j|^n, (\sum_{j=1}^{i} |h_j|)^m \le i^{m-1} \sum_{j=1}^{i} |h_j|^m \tag{13}$$

3. Design and analysis

3.1 Fixed-time adaptive NNs Sliding Mode Control

In this section, we can divide it into three steps. First, design the non-singular fast terminal sliding function and verify stability. Secondly, introduce the double-power approach rate and give proof of the fixed-time convergence. Finally, design the RBFNNs adaptive law, and then we design the Lyapunov function to prove that the system can achieve fixed-time convergence.

Assume an uncertain nonlinear second-order system (1), to enable x to track x_d, design error function as

$$\begin{cases} e_1 = x_1 - x_d \\ \dot{e}_1 = e_2 = \dot{x}_1 - \dot{x}_d \\ \dot{e}_2 = \dot{x}_2 - \ddot{x}_d \end{cases} \tag{14}$$

Design NFTSM function as

$$s = e_1 + \alpha |e_1|^{p_1} sign(e_1) + \beta |e_2|^{p_2} sign(e_2) \tag{15}$$

Where $\alpha > 0, \beta > 0, 1 < p_2 < 2, p_1 > p_2, p_1 = \frac{g}{h}$

$p_2 = \frac{z}{l}, g, h, z, l \in N$ are odd numbers.

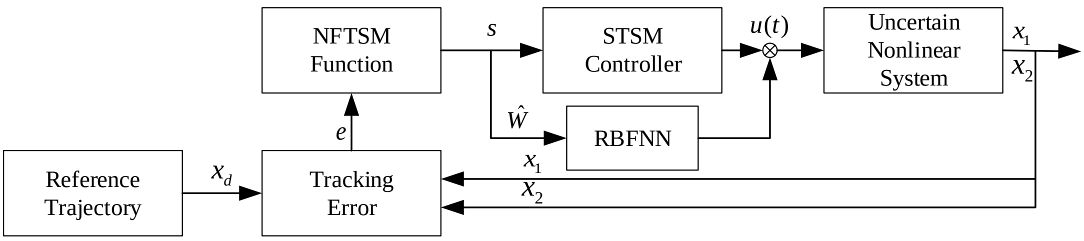

Fig. 2. Control flowchart of second-order nonlinear system

Proof 1: The low order of e_1 plays a leading role and tends to the equilibrium point. The law of system state change on the sliding surface is

$$\beta|e_2|^{p_2}\, sign(e_2) = -e_1$$
$$\dot{e}_1 = e_2 = -sign(e_1)(\frac{e_1}{\beta})^{\frac{1}{p_2}}, (0 < \frac{1}{p_2} < 1) \tag{16}$$

The higher order of e_1 plays a leading role and tends to the equilibrium point. The system state change law on the sliding surface is

$$\beta|e_2|^{p_2}\, sign(e_2) = -\alpha|e_1|^{p_1}\, sign(e_1)$$
$$\dot{e}_1 = e_2 = -sign(e_1)\left(\frac{\alpha|e_1|^{p_1}}{\beta}\right)^{\frac{1}{p_2}}, (\frac{p_1}{p_2} > 1) \tag{17}$$

There have been a large number of results showing the verification of finite time convergence(Liu et al., 2018) ,and then the finite time convergence conclusion obtained by simply analogy with the law of constant velocity approximation

When $e_1 \gg 1$

$$\dot{e}_1 = -k_1 sign(e_1)|e_1|^{n_1}, n_1 > 1 \tag{18}$$

Compared with the isokinetic approach rate

$$-k_1 sign(e_1)|e_1|^{n_1} < -k \tag{19}$$

This shows that the NFTSM has a faster convergence rate than the constant velocity approach rate when it is far from the equilibrium point.

When $0 < e_1 \ll 1$

$$\dot{e}_1 = -k_2 sign(e_1)|e_1|^{n_2}, n_2 < 1 \tag{20}$$

Compared with the isokinetic approach rate

$$-k_2 sign(e_1)|e_1|^{n_2} < -k \tag{21}$$

This shows that the NFTSM has a faster convergence rate when approaching the equilibrium point than the constant velocity approach rate. Through the above analysis, it can be seen that $\dot{e}_1 = -k$ can make the system error converges to 0 in finite time, so that the NFTSM surface determined by the formula can quickly converge to 0 in finite time. Proof completed.

In the next step, we can design and analyze the controller according to the control strategy in Fig.2.

According to (15) we can get

$$\dot{s} = e_2 + p_1\alpha|e_1|^{p_1-1} e_2 + p_2\beta|e_2|^{p_2-1}(f(x) + \Lambda u + d_t - \ddot{x}_d) \tag{22}$$

To achieve the estimated synovial surface, the equivalent control law is designed without considering interference conditions

$$u_{eq} = \frac{1}{\Lambda}(-f(x) + \ddot{x}_d - \frac{|e_2|^{2-p_2}(1 + p_1\alpha|e_1|^{p_1-1})}{p_2\beta}) \tag{23}$$

We use the dual-power sliding mode approach rate as the switching control law as

$$u_{sw} = \dot{s} = -k_1|s|^{w_1} sign(s) - k_2|s|^{w_2} sign(s) \tag{24}$$

Where $k_1 > 0, k_2 > 0, 0 < w_1 < 1, w_2 > 1$, the final control law is

$$u = u_{eq} + u_{sw} \tag{25}$$

$$u = \frac{1}{\Lambda}(-f(x) + \ddot{x}_d - \frac{|e_2|^{2-p_2}(1 + p_1\alpha|e_1|^{p_1-1})}{p_2\beta}) - k_1|s|^{w_1} sign(s) - k_2|s|^{w_2} sign(s) \tag{26}$$

However, there is an unknown $f(x)$ in the mathematical model of the second-order nonlinear system, so the control law (26) cannot completely achieve the superior control effect. Therefore, this paper will use RBFNNs to approximate the nonlinear part, which can effectively enhance the robust performance of the nonlinear system.

As a feedforward NN, the RBFNN has the best approximation effect and does not have the advantages of local minima and fast learning convergence, the schematic diagram of the structure of the

RBFNN is shown in Fig. 3. Therefore, it has been used in a large number of academic researches and has been effectively verified (Zhang et al., 2020c). RBFNNs are used to design NNs control.

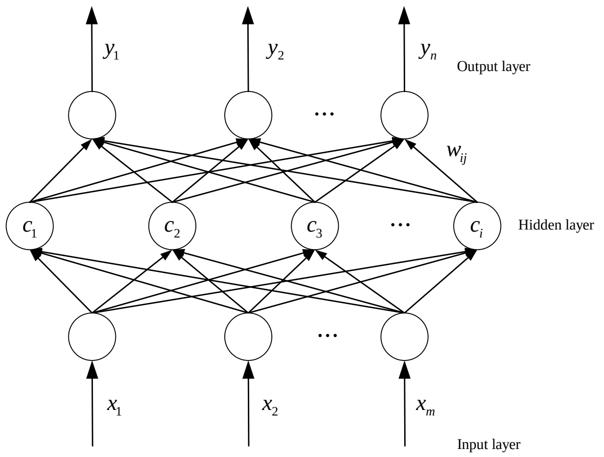

Fig. 3. RBFNNs structure diagram.

Choosing a NN controller

$$u = \frac{1}{\Lambda}\left(-\hat{f} + \ddot{x}_d - \frac{|e_2|^{2-p_2}(1+p_1\alpha|e_1|^{p_1-1})}{p_2\beta}\right) \\ -k_1|s|^{w_1}\, sign(s) - k_2|s|^{w_2}\, sign(s) \tag{27}$$

Where $\hat{f} = \hat{W}^T h(x)$ -NNs output.

The sliding surface of the nonlinear system can be written as

$$\dot{s} = e_2 + p_1\alpha|e_1|^{p_1-1} e_2 + p_2\beta|e_2|^{p_2-1}(\Lambda u \\ + f(x) + d_t - \ddot{x}_d) \tag{28}$$

Where

$$f^* = f(x) + d_t = W^*\Psi(x) + \varepsilon \tag{29}$$

Calculate the approximate error of the system model as

$$\tilde{f} = f^* - \hat{f} = W^{*T}h(x) + \varepsilon - \hat{W}^T h(x) \\ = \tilde{W}^T h(x) + \varepsilon \tag{30}$$

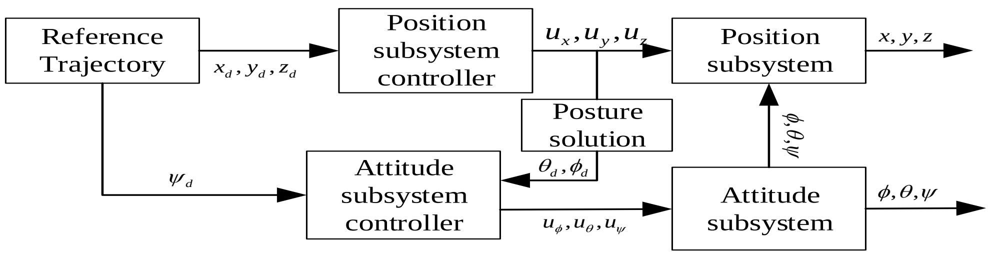

Fig.4 Structure diagram of the quadrotor control system

According to the controller (26) and the sliding function (28), we can get

$$\dot{s} = p_2\beta|e_2|^{p_2-1}(\tilde{W}^T h(x) + \varepsilon - k_1|s|^{w_1}\, sign(s) \\ -k_2|s|^{w_2}\, sign(s)) \tag{31}$$

Where $k_1 > 0, k_2 > 0$, to achieve fixed-time convergence, we choose $w_1 + w_2 = 2$ and $w_1 = \frac{1}{3}, w_2 = \frac{5}{3}$.

Theorem 1: For system (24), when $w_1 + w_2 = 2$, it can reach the fixed time convergence. It can also be considered that there is $u_{sw} = \dot{u}_{sw} = 0$ after the finite time convergence T and the convergence time T has an upper bound $T_{\sup}$ that has nothing to do with the initial state value $u_{sw}0$, where

$$T = \frac{1}{\sqrt{k_1k_2}(1-w_2)}\arctan\left(\sqrt{\frac{k_1}{k_2}}|s0|^{1-w_2}\right) \\ T_{\sup} = \frac{\pi}{2\sqrt{k_1k_2}(1-w_2)} \tag{32}$$

Proof 2: When $s > 0$, and $w_1 + w_2 = 2$, system (24) can get the following equation as

$$\dot{s} + k_1 s^{2-w_2} + k_2 s^{w_2} = 0 \tag{33}$$

Then, equation (33) divided by s^{w_2} on both sides of the equal sign, we can get

$$s^{-w_2}\dot{s} + k_1 s^{2-2w_2} + k_2 = 0 \tag{34}$$

In the next step, we set $\Upsilon = s^{1-w_2}$, then $s = \Upsilon^{\frac{1}{1-w_2}}$, and substitute u_{sw} into equation (34), we can get the generalized Riccati differential equation as

$$\dot{\Upsilon} + (1-w_2)k_1\Upsilon^2 + (1-w_2)k_2 = 0 \tag{35}$$

Then, we can get the general solution of equation (35)as

$$\Upsilon = \sqrt{\frac{k_2}{k_1}}\tan\left[T_0 - \sqrt{k_1k_2}(1-w_2)t\right] \tag{36}$$

Get from $s(0) = s0$ as

$$u_{sw}=\begin{cases} sign(s0)\left[\sqrt{k_1/k_2}\tan(T_0-ct)\right]^{\frac{1}{1-w_2}}, t\le \frac{T_0}{c} \\ 0, t>\dfrac{\arctan(\sqrt{k_1/k_2}\left|s0\right|^{1-w_2}}{\sqrt{k_1k_2}(1-w_2)} \end{cases} \tag{37}$$

Therefore, the convergence time is

$$T=\frac{T_0}{c}=\frac{1}{\sqrt{k_1k_2}(1-w_2)}\arctan(\sqrt{\frac{k_1}{k_2}}\left|s0\right|^{1-w_2}) \tag{38}$$

From equation (38) we can find that the initial value $s0$ only appears in the arctangent function $\arctan(\sqrt{\frac{k_1}{k_2}}\left|s0\right|^{1-w_2})$, and the value interval $\arctan(x)\in\left[0,\frac{\pi}{2}\right], x\ge 0$ can be obtained from the arctangent function

$$T<T_{\sup}=\frac{\pi}{2\sqrt{k_1k_2}(1-w_2)} \tag{39}$$

Therefore, the convergence rate (24) has an upper limit of $T_{\sup}$ at $w_1+w_2=2$ and has nothing to do with the initial value $s0$. Proof completed.

Proof 3: Select Lyapunov candidate function

$$V_S=\frac{1}{2}s^2 \tag{40}$$

$$\begin{aligned}\dot{V}_S=s\dot{s}=sp_2\beta\left|e_2\right|^{p_2-1}sign(e_2)(\tilde{W}^Th(x)+\varepsilon\\ -k_1\left|s\right|^{\frac{1}{3}}sign(s)-k_2\left|s\right|^{\frac{5}{3}}sign(s))\end{aligned} \tag{41}$$

Select Lyapunov candidate function

$$V_{NN}=\frac{1}{2}\tilde{W}^T\xi\tilde{W}, \xi=\xi^T>0 \tag{42}$$

$$\begin{aligned}\dot{V}_{NN}=-\tilde{W}^T(sp_2\beta\left|e_2\right|^{p_2-1}h(x)-\sigma_z\hat{W}^\nu\\ -\sigma_x\hat{W}^\gamma)\end{aligned} \tag{43}$$

Where

$$\dot{\hat{W}}=\xi^{-1}\left[sp_2\beta\left|e_2\right|^{p_2-1}h(x)-\sigma_z\hat{W}^\nu-\sigma_x\hat{W}^\gamma\right] \tag{44}$$

Select Lyapunov function

$$V=V_s+V_{NN} \tag{45}$$

$$\begin{aligned}\dot{V}&=\dot{V}_s+\dot{V}_{NN}\\ &=sp_2\beta\left|e_2\right|^{p_2-1}(\tilde{W}^Th(x)+\varepsilon\\ &-k_1\left|s\right|^{\frac{1}{3}}sign(s)-k_2\left|s\right|^{\frac{5}{3}}sign(s))+\dot{V}_{NN}\end{aligned} \tag{46}$$

$$\begin{aligned}\dot{V}&=\dot{V}_s+\dot{V}_{NN}\\ &=sp_2\beta\left|e_2\right|^{p_2-1}(\tilde{W}^Th(x)\\ &+\varepsilon-k_1\left|s\right|^{\frac{1}{3}}sign(s)-k_2\left|s\right|^{\frac{5}{3}}sign(s))\\ &-\tilde{W}^T\xi(\xi^{-1}[sp_2\beta\left|e_2\right|^{p_2-1}h(x)\\ &-\sigma_z\hat{W}^\nu-\sigma_x\hat{W}^\gamma])\\ &=sp_2\beta\left|e_2\right|^{p_2-1}\varepsilon\\ &+sp_2\beta\left|e_2\right|^{p_2-1}(-k_1\left|s\right|^{\frac{1}{3}}sign(s)\\ &-k_2\left|s\right|^{\frac{5}{3}}sign(s))-\sigma_z\tilde{W}^T\hat{W}^\nu-\sigma_x\tilde{W}^T\hat{W}^\gamma\end{aligned} \tag{47}$$

According to Lemma 2 and Lemma 3, the following inequalities can be established

$$\begin{aligned}&-\sigma_z\tilde{W}^T\hat{W}^\nu\le\\ &-\sigma_1(\frac{1}{2}\tilde{W}^T\xi^{-1}\tilde{W})^{\frac{1+\nu}{2}}+\sigma_2W^{*\frac{1+\nu}{2}T}W^{*\frac{1+\nu}{2}}\end{aligned} \tag{48}$$

$$\begin{aligned}&-\sigma_x\tilde{W}^T\hat{W}^\gamma\le\\ &-\sigma_3(\frac{1}{2}\tilde{W}^T\xi^{-1}\tilde{W})^{\frac{1+\gamma}{2}}+\sigma_4W^{*\frac{1+\gamma}{2}T}W^{*\frac{1+\gamma}{2}}\end{aligned} \tag{49}$$

$$s\varepsilon\le\frac{1}{\nu+1}s^{\nu+1}+\frac{\nu}{\nu+1}\varepsilon^{\frac{\nu+1}{\nu}} \tag{50}$$

Where $\sigma_1>0,\sigma_2>0,\sigma_3>0,\sigma_4>0$, then we have

$$\begin{aligned}\dot{V}&=\dot{V}_s+\dot{V}_{NN}\\ &\le p_2\beta(\frac{1}{\nu+1}s^{\nu+1}+\frac{\nu}{\nu+1}\varepsilon^{\frac{\nu+1}{\nu}}-k_1\left|s\right|^{\frac{4}{3}}-k_2\left|s\right|^{\frac{8}{3}})\\ &-\sigma_1(\frac{1}{2}\tilde{W}^T\xi^{-1}\tilde{W})^{\frac{1+\nu}{2}}+\sigma_2W^{*\frac{1+\nu}{2}T}W^{*\frac{1+\nu}{2}}\\ &-\sigma_3(\frac{1}{2}\tilde{W}^T\xi^{-1}\tilde{W})^{\frac{1+\gamma}{2}}+\sigma_4W^{*\frac{1+\gamma}{2}T}W^{*\frac{1+\gamma}{2}}\\ &\le\Gamma(\frac{1}{2}s^2)^{\frac{\nu+1}{2}}-\vartheta(\frac{1}{2}s^2)^{\frac{\gamma+1}{2}}-\sigma_1(\frac{1}{2}\tilde{W}^T\xi^{-1}\tilde{W})^{\frac{1+\nu}{2}}\\ &+\sigma_2W^{*\frac{1+\nu}{2}T}W^{*\frac{1+\nu}{2}}-\sigma_3(\frac{1}{2}\tilde{W}^T\xi^{-1}\tilde{W})^{\frac{1+\gamma}{2}}\\ &+\sigma_4W^{*\frac{1+\gamma}{2}T}W^{*\frac{1+\gamma}{2}}+p_2\beta\frac{\nu}{\nu+1}\varepsilon^{\frac{\nu+1}{\nu}}\end{aligned} \tag{51}$$

$$\Gamma=2^{\frac{\nu+1}{2}}p_2\beta(\frac{1}{\nu+1}-k_1), \vartheta=2^{\frac{\gamma+1}{2}}p_2\beta k_2 \tag{52}$$

According to Lemma 4, then we can get

$$\begin{aligned}\dot{V}&\le\Gamma(V_s)^{\frac{\nu+1}{2}}-\vartheta(V_s)^{\frac{\gamma+1}{2}}-\sigma_1V_{NN}^{\frac{1+\nu}{2}}\\ &+\sigma_2W^{*\frac{1+\nu}{2}T}W^{*\frac{1+\nu}{2}}-\sigma_3V_{NN}^{\frac{1+\gamma}{2}}\\ &+\sigma_4W^{*\frac{1+\gamma}{2}T}W^{*\frac{1+\gamma}{2}}+p_2\beta\frac{\nu}{\nu+1}\varepsilon^{\frac{\nu+1}{\nu}}\\ &\le-\varsigma_xV^{\frac{\nu+1}{2}}-\delta_xV^{\frac{\gamma+1}{2}}+\partial_x\end{aligned} \tag{53}$$

Where

$$\begin{aligned}
&\varsigma_x = \min\left(-\Gamma, 2^{\frac{\nu+1}{2}}\sigma_{px}\right) \\
&\delta_x = \min\left(\vartheta, 2^{\frac{\gamma+1}{2}}\sigma_{pz}\right) \\
&\partial_x = \sigma_2 W^{*\frac{1+\nu}{2}T} W^{*\frac{1+\nu}{2}} + \sigma_4 W^{*\frac{1+\gamma}{2}T} W^{*\frac{1+\gamma}{2}} \\
&\quad + p_2\beta\frac{\nu}{\nu+1}\varepsilon^{\frac{\nu+1}{\nu}}
\end{aligned} \tag{54}$$

Then, according to Lemma 1, the system is approximately stable in fixed-time, and the convergence time is

$$T_{x\max} = \frac{2^{\frac{3-\nu}{2}}}{(1-\nu)\varsigma_x} + \frac{2}{(\gamma-1)\delta_x}$$

Where $\nu = \frac{1}{3}, \gamma = \frac{5}{3}$, $\Gamma < 0, \vartheta > 0$, σ_{px} and σ_{pz} deponds on ν, γ.

Proof completed.

Remark 2: To verify that the theorem obtained in this paper is not limited to simple uncertain nonlinear systems, the theorem will be applied to the tracking control of quadrotor UAVs in the next section.

3.2 Application and Analysis of Tracking Control of Quadrotor Aircraft

Considering that the actual working dynamic model of the quadrotor is a typical uncertain under-actuated nonlinear system. In this section, we will apply the algorithm theorem proposed in the previous section to analyze the quadrotor UAV system model.

In this paper, the attitude calculation is used to obtain the target attitude angle of the quadrotor UAV. Assuming expectation $\psi_d = 0$, after the attitude calculation of the position subsystem, ϕ_d, θ_d can be obtained, so as to achieve tracking control(Chen et al., 2016).

$$\phi_d = \arcsin\left(\frac{P_x \sin(\psi_d) - P_y \cos(\psi_d)}{\sqrt{P_x^2 + P_y^2 + P_z^2}}\right) \tag{55}$$

$$\theta_d = \arctan\left(\frac{P_x \cos(\psi_d) + P_y \sin(\psi_d)}{P_z}\right) \tag{56}$$

Where $u_1 = \|u_s\| = \sqrt{P_x^2 + P_y^2 + P_z^2}$.

Theorem 2: Taking into account the quadrotor UAV system (2)(3), system tracking error (14), sliding mode surface (15) and approach rate (24), we can get the tracking virtual control law of the position subsystem.

$$\begin{aligned}
u_x &= A^{-1}(-\hat{W}_1^T h_1(x) + \ddot{x}_d \\
&\quad - \frac{|e_2|^{2-p_2}(1 + p_1\alpha|e_1|^{p_1-1})}{p_2\beta}) \\
&\quad - k_1|s_x|^{\frac{1}{3}} sign(s_x) - k_2|s_x|^{\frac{5}{3}} sign(s_x)
\end{aligned} \tag{57}$$

$$\begin{aligned}
\dot{\hat{W}}_1 &= \xi^{-1}(sp_2\beta|z_2|^{p_2-1} h_1(x) \\
&\quad - \sigma_z \hat{W}^{\nu} - \sigma_x \hat{W}^{\gamma})
\end{aligned} \tag{58}$$

Where $u_x = \left[P_x, P_y, P_z\right]^T$ is the virtual control input on the position of the quadrotor UAV, and $\dot{\hat{W}}_1$ is the fixed-time adaptive law.

Theorem 3: In the same way, we can get the virtual controller of the attitude subsystem. Then we have

$$\begin{aligned}
u_p &= B^{-1}(-\hat{W}_2^T h_2(x) + \ddot{p}_d \\
&\quad - \frac{|e_2|^{2-p_2}(1 + p_1\alpha|e_1|^{p_1-1})}{p_2\beta}) \\
&\quad - k_1|s_p|^{\frac{1}{3}} sign(s_p) - k_2|s_p|^{\frac{5}{3}} sign(s_p)
\end{aligned} \tag{59}$$

$$\begin{aligned}
\dot{\hat{W}}_2 &= \xi^{-1}(sp_2\beta|z_4|^{p_2-1} h_2(x) \\
&\quad - \sigma_z \hat{W}^{\nu} - \sigma_x \hat{W}^{\gamma})
\end{aligned} \tag{60}$$

Where $z_1 = x_1 - x_d, z_2 = \dot{x}_1 - \dot{x}_d, z_3 = p_1 - p_d, z_4 = \dot{p}_1 - \dot{p}_d$ is the tracking error function of the system. $u_p = \left[u_\phi, u_\theta, u_\psi\right]^T$ is the control input on the attitude of quadrotor UAVs, and $\dot{\hat{W}}_2$ is the fixed-time adaptive law.

Remark 3: According to the proof in the previous section, it is easy to draw the same conclusion, so to avoid repeated descriptions, it will not be given.

4. Result

In this section, simulations are performed to verify the effectiveness of the proposed fixed-time adaptive NN sliding mode control for uncertain nonlinear systems. And the algorithm is applied to a quadrotor UAV, to verify the effective performance and anti-interference ability of the algorithm in complex nonlinear systems. In the comparative experiment, the most critical attitude robustness in the work of a quadrotor UAV was verified.

4.1 Simulation and verification of uncertain nonlinear systems

For the nonlinear system (1), the reference trajectory is given as

$$x_d = \sin(t)$$

The controller and network parameters are selected as

$$k_1 = 3000, k_2 = 0.1, \alpha = 50, \beta = 3$$

$$p_1 = \frac{3}{2}, p_2 = \frac{5}{3}, b = 20, \sigma_z = \sigma_x = 2$$

$$f(x) = \cos(x_1), \Lambda = 1, dt = 0.1\sin(t)$$

The initial conditions of the system are

$$x_1 = 0.5, \dot{x}_1 = x_2 = 0$$

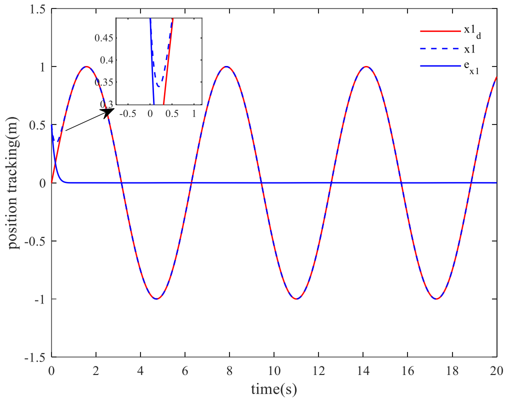

Fig.5 Position tracking control and error.

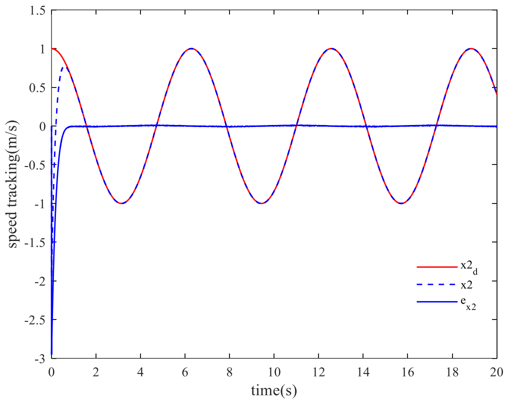

Fig.6 Speed tracking control and error.

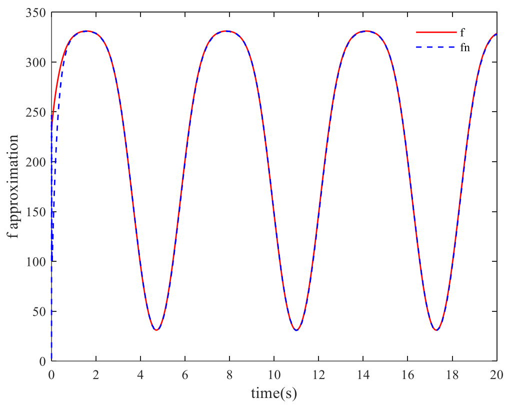

Fig.7 Trajectories of NNs

Fig.5-Fig.7 verify the effectiveness of the algorithm in dealing with uncertain nonlinear systems, and the maximum time to reach system stability is $T_{x\max} = 5.742$.

4.2 Simulation of tracking control of Quadrotor UAVs

In this section, a numerical example is performed to verify the tracking control of the quadrotor UAV.

In simulations B and C, we select the parameters of the quadrotor, initial conditions, and reference trajectories $x_d(t) = [x_d(t), y_d(t), z_d(t)]^T$ and $\psi_d = 0$ of the system are as follows

$$m = 2, l = \frac{1}{5}, g = 9.8, \xi_x = \xi_y = \xi_z = \frac{6}{5}$$

$$\xi_\phi = \xi_\theta = \xi_x = \frac{6}{5}, I_x = I_y = 1.25, I_z = 2.5$$

$$x_d(t) = \left[5\left(1-\cos\left(\frac{\pi}{10}t\right)\right), 5\sin\left(\frac{\pi}{10}t\right), 10\left(1-e^{-\frac{3}{10}t}\right)\right]^T$$

$$\phi_d = \arcsin\left(\frac{P_x \sin(\psi_d) - P_y \cos(\psi_d)}{\sqrt{P_x^2 + P_y^2 + P_z^2}}\right)$$

$$\theta_d = \arctan\left(\frac{P_x \cos(\psi_d) + P_y \sin(\psi_d)}{P_z}\right)$$

$$x(0) = y(0) = z(0) = \phi(0) = \theta(0) = \psi(0) = 0.5$$

The position subsystem controller and network parameters are

$$k_1 = 15, k_2 = 0.1, \alpha = 50, \beta = 1, p_1 = \frac{7}{3}$$

$$p_2 = \frac{5}{3}, \quad b = 5, \sigma_z = \sigma_x = 2, d_a = 0.1\sin(t)$$

Remark 4. The parameters of the three virtual controllers are the same, so we will not describe them.

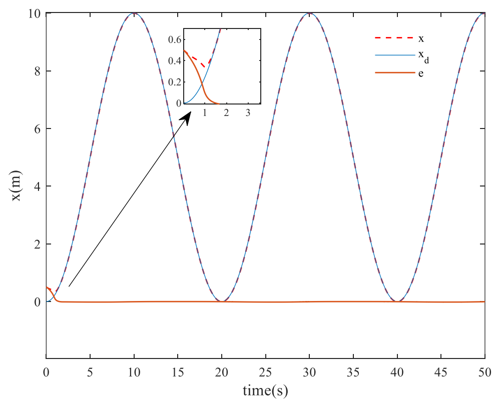

Fig.8 x tracks the reference trajectory x_d ,and the tracking error e .

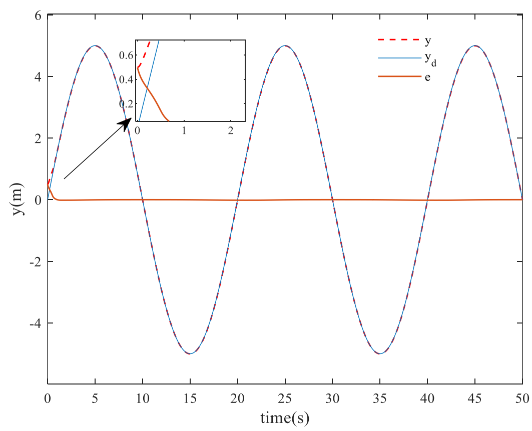

Fig.9 y tracks the reference trajectory y_d and the tracking error e .

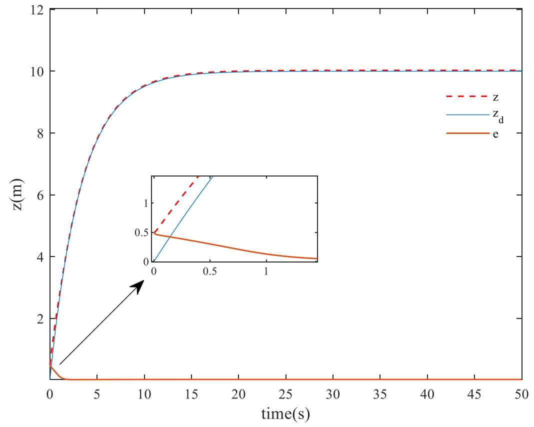

Fig. 10 z tracks the reference trajectory z_d and the tracking error e.

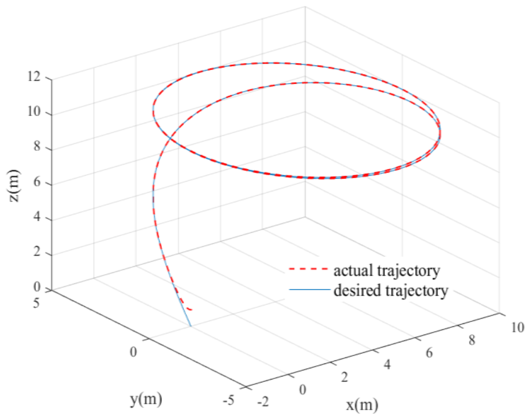

Fig.11 3-D space states tracking result

The attitude subsystem controller and network parameters are shown in Table 1.

Table1. Attitude subsystem controller parameters

ϕ	$k_1 = 400, k_2 = 0.1, p_1 = \frac{7}{3}$ $p_2 = \frac{5}{3}, \alpha_1 = 50, \beta_1 = 5, \sigma_z = \sigma_x = 2$
θ	$k_1 = 400, k_2 = 0.1, p_1 = \frac{7}{3}, p_2 = \frac{5}{3}$ $\alpha_1 = 10, \beta_1 = 1, \sigma_z = \sigma_x = 2$
ψ	$k_1 = 400, k_2 = 1, p_1 = \frac{7}{3}, p_2 = \frac{5}{3}$ $\alpha_1 = 10, \beta_1 = 1, \sigma_z = \sigma_x = 2$
interference	$d_i = 0.1\sin(t), i = (\phi, \theta, \psi)$

According to Fig.8-Fig.14, the effectiveness of the algorithm in the quadrotor UAV can be obtained, and the fitting effect of the NN is shown in Fig.15-Fig.16. The control input of a quadrotor UAV is shown in Fig.17.According to Lemma 1, the maximum convergence time of three positions $T_{x\max} = T_{y\max} = T_{z\max} = 5.513$ and the maximum convergence time of three postures $T_{\phi\max} = 1.7209$, $T_{\theta\max} = 5.5232$ $T_{\psi\max} = 5.5232$ can be obtained. According to the simulation results, we can find that the system can quickly reach stability and has a good tracking effect.

C. Comparison and verification of the robustness of UAVs attitude control

In this section, the robust performance of two different control strategies in quad-rotor attitude control is verified.

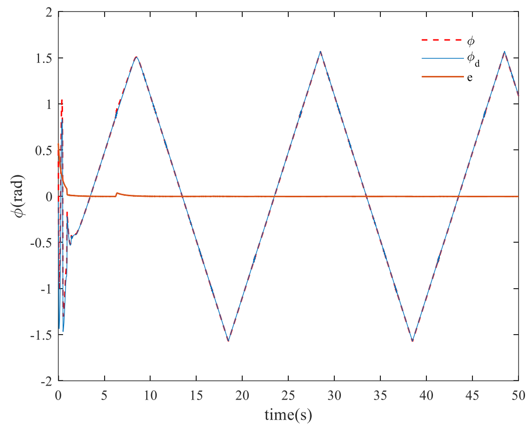

Fig.12 ϕ tracks the reference trajectory ϕ_d and the tracking error e.

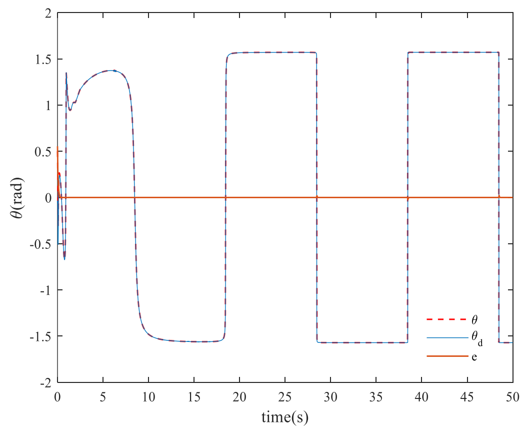

Fig.13 θ tracks the reference trajectory θ_d and the tracking error e.

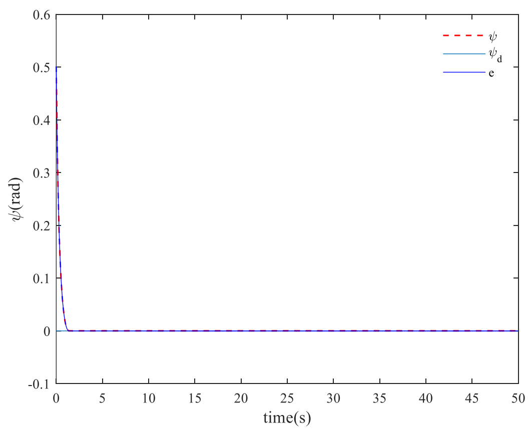

Fig.14 ψ tracks the reference trajectory ψ_d and the tracking error e.

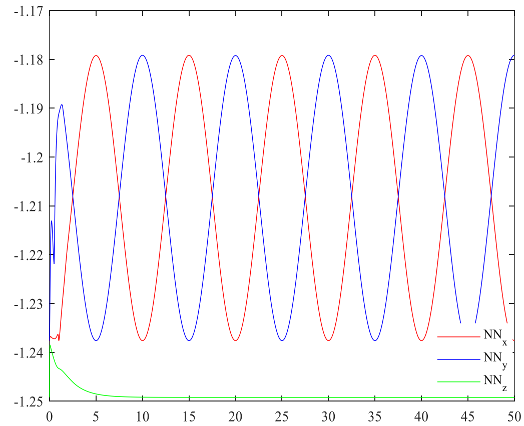

Fig.15 The trajectory of the NN of the position subsystem

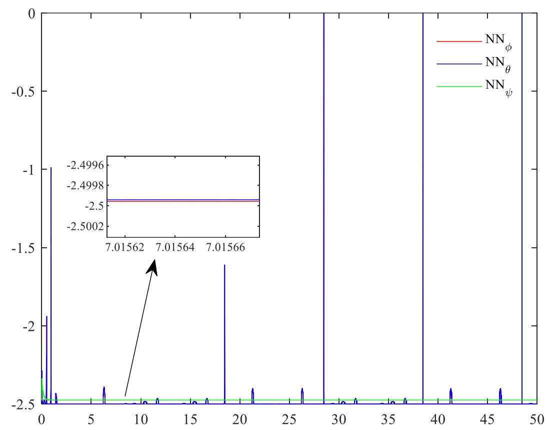

Fig.16 The trajectory of the posture subsystem NN

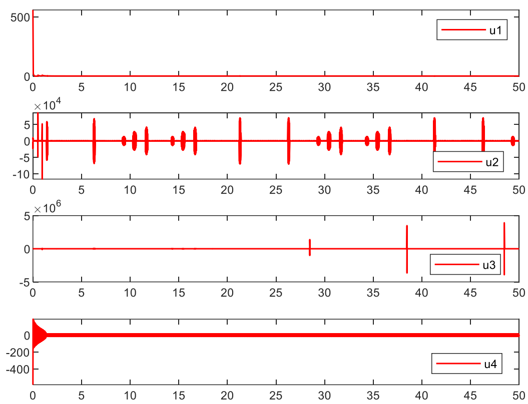

Fig.17 Controller input.

Case 1(Fixed-time adaptive NNs sliding mode control) We first design a non-singular fast terminal dual-power sliding mode control law, and then give a fixed-time RBFNNs control law, and finally apply it to the attitude tracking control of the quadrotor.

Case2(Non-singular fast terminal Super-Twisting sliding mode control(Alqaisi et al., 2020):)

To verify the anti-interference advantage of the fixed-time adaptive NNs, the algorithm is used for comparison in the tracking control of the quadrotor UAVs.

When interference $d_t = 50\sin(\phi t)$ is added at $t > 20$, the simulation parameters and results are as follows

$$k_1 = 15, k_2 = 0.01, \alpha = 50, \beta = 1, p_1 = \frac{7}{3}$$

$$p_2 = \frac{5}{3}, \quad b = 5, \sigma_z = \sigma_x = 2$$

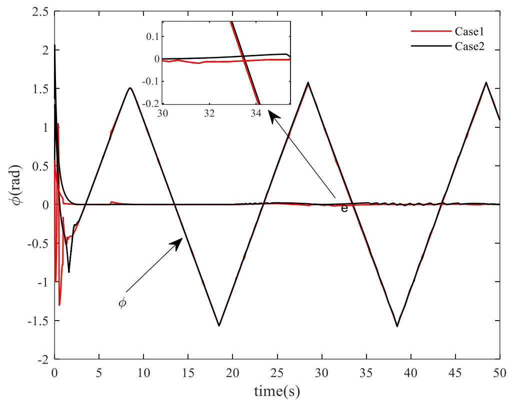

Fig.17 Comparison of the results of case1 and case2 ϕ .

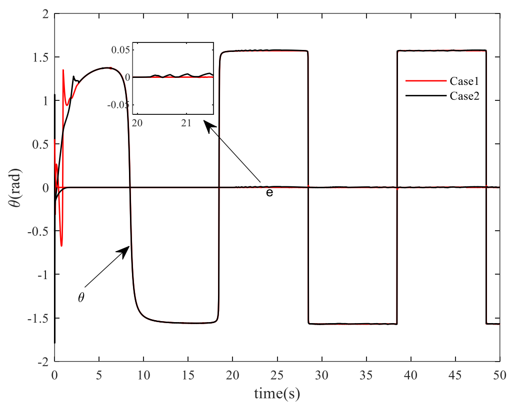

Fig.18 Comparison of the results of case1 and case2 θ .

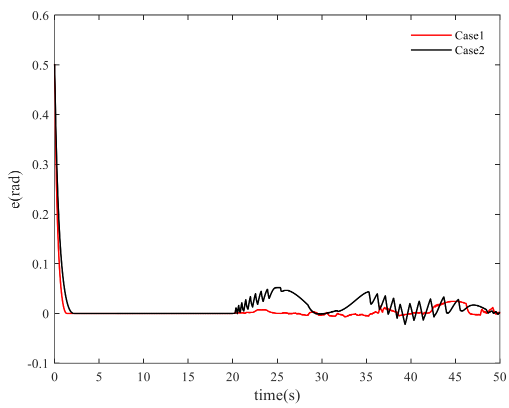

Fig.19 Comparison of the results of case1 and case2 ψ .

According to the comparison between Fig.17-Fig.19, we get that the algorithm has stronger robustness and convergence speed in the attitude control of quadrotor UAVs. When $t > 20$, case1 has higher convergence performance than case2 under the same interference conditions. After comparison, we can conclude that the algorithm proposed in this paper can resist large interference and remain stable.

5. Conclusion

In this paper, the fixed-time NN adaptive control technology based on the non-singular fast terminal dual-power sliding mode algorithm provides a highly robust control strategy for nonlinear systems and is verified by an example in a quadrotor UAV tracking control for the first time. The state of the weight system of the RBFNNs can guarantee convergence in a fixed time, regardless of the state. The simulation results show that the fixed-time controller proposed in this paper can ensure that the nonlinear system converges in finite time when only the controller parameters are considered, and it has the superior robust performance. The verification of the numerical example shows the effectiveness and high robustness of the adaptive fixed-time NN sliding mode control method.

References

Khalil H. Nonlinear Systems / H.K. Khalil [J]. 2020.

Yao L, You S, Xiaodong L, et al. Control allocation for a class of morphing aircraft with integer constraints based on Lévy flight [J]. Journal of Systems Engineering and Electronics, 2020, 31(4): 826-40.

Li T S, Kuo P, Ho Y, et al. Intelligent Control Strategy for Robotic Arm by Using Adaptive Inertia Weight and Acceleration Coefficients Particle Swarm Optimization [J]. IEEE Access, 2019, 7(126929-40.

Wang Y, Shan M, Wang D. Motion Capability Analysis for Multiple Fixed-Wing UAV Formations With Speed and Heading Rate Constraints [J]. IEEE Transactions on Control of Network Systems, 2020, 7(2): 977-89.

Zhihua Q, Hull R A, Jing W. Globally stabilizing adaptive control design for nonlinearly-parameterized systems [J]. IEEE Transactions on Automatic Control, 2006, 51(6): 1073-9.

Krishnamurthy P, Lu W, Khorrami F, et al. Robust Force Control of an SRM-Based Electromechanical Brake and Experimental Results [J]. IEEE Transactions on Control Systems Technology, 2009, 17(6): 1306-17.

Franco P D, Scarciotti G, Astolfi A. Stability of nonlinear differential-algebraic systems via additive identity [J]. IEEE/CAA Journal of Automatica Sinica, 2020, 7(4): 929-41.

Bi X, Shi X. Attitude stabilization of rigid spacecraft implemented in backstepping control with input delay [J]. Journal of Systems Engineering and Electronics, 2017, 28(5): 955-62.

Li Z, Xia Y, Su C, et al. Missile Guidance Law Based on Robust Model Predictive Control Using Neural-Network Optimization [J]. IEEE Transactions on Neural Networks and Learning Systems, 2015, 26(8): 1803-9.

Fujimoto K, Sakata N, Maruta I, et al. A Passivity Based Sliding Mode Controller for Simple Port-Hamiltonian Systems [J]. IEEE Control Systems Letters, 2021, 5(3): 839-44.

Wang A, Liu L, Qiu J, et al. Event-Triggered Robust Adaptive Fuzzy Control for a Class of Nonlinear Systems [J]. IEEE Transactions on Fuzzy Systems, 2019, 27(8): 1648-58.

Zeng Lian L, Svoboda J. A new control scheme for nonlinear systems with disturbances [J]. IEEE Transactions on Control Systems Technology, 2006, 14(1): 176-81.

Chen M, Chen C. Robust Nonlinear Observer for Lipschitz Nonlinear Systems Subject to Disturbances [J]. IEEE Transactions on Automatic Control, 2007, 52(12): 2365-9.

Yin C, Xu J, Hou Z. A High-Order Internal Model Based Iterative Learning Control Scheme for Nonlinear Systems With Time-Iteration-Varying Parameters [J]. IEEE Transactions on Automatic Control, 2010, 55(11): 2665-70.

Guifang L, Chen Y. Controller design for stochastic nonlinear systems with matched conditions [J]. Journal of Systems Engineering and Electronics, 2018, 29(1): 160-5.

Li Y X, Hou Z, Che W W, et al. Event-Based Design of Finite-Time Adaptive Control of Uncertain Nonlinear Systems [J]. IEEE Transactions on Neural Networks and Learning Systems, 2021, 1-10.

Zhang Y, Wang F. Observer-Based Fixed-Time Neural Control for a Class of Nonlinear Systems [J]. IEEE Transactions on Neural Networks and Learning Systems, 2021, 1-11.

Huang C, Chen J, Chen C, et al. Geological Segmentation on UAV Aerial Image Using Shape-Based LSM with Dominant Color; proceedings of the 2016 30th International Conference on Advanced Information Networking and Applications Workshops (WAINA), F 23-25 March 2016, 2016 [C].

Ma F, Xu Z, Xiong F. Research on Route Planning of Plant Protection UAV Based on Area Modular Division; proceedings of the 2019 11th International Conference on Intelligent Human-Machine Systems and Cybernetics (IHMSC), F 24-25 Aug. 2019, 2019 [C].

Mintchev S, Floreano D. A pocket sized foldable quadcopter for situational awareness and reconnaissance; proceedings of the 2016 IEEE International Symposium on Safety, Security, and Rescue Robotics (SSRR), F 23-27 Oct. 2016, 2016 [C].

Kim S, Ahn C K. Auto-Tuner-Based Controller for Quadcopter Attitude Tracking Applications [J]. IEEE Transactions on Circuits and Systems II: Express Briefs, 2019, 66(12): 2012-6.

Santoso F, Garratt M A, Anavatti S G, et al. Robust Hybrid Nonlinear Control Systems for the Dynamics of a Quadcopter Drone [J]. IEEE Transactions on Systems, Man, and Cybernetics: Systems, 2020, 50(8): 3059-71.

Wu X, Zhang J, Zhu Q. A generalized procedure in designing recurrent neural network identification and control of time-varying-delayed nonlinear dynamic systems [J]. Neurocomputing, 2009, 73(7):

Salt L, Howard D, Indiveri G, et al. Parameter Optimization and Learning in a Spiking Neural Network for UAV Obstacle Avoidance Targeting Neuromorphic Processors [J]. IEEE Transactions on Neural Networks and Learning Systems, 2020, 31(9): 3305-18.

Wu Y-Y, Zhang Y, Wu A-G. Preassigned finite-time attitude control for spacecraft based on time-varying barrier Lyapunov functions [J]. Aerospace Science and Technology, 2021, 108(106331.

Gao Z, Guo G. Command filtered finite-time formation tracking control of AUVs with unknown control directions [J]. IET Control Theory & Applications, 2020, 14(13): 1744-51.

Yang Y, Niu Y. Fixed-time adaptive fuzzy control for uncertain non-linear systems under event-triggered strategy [J]. IET Control Theory & Applications, 2020, 14(14): 1845-54.

Wang Y, Cai H, Zhang J, et al. Disturbance Attenuation Predictive Optimal Control for Quad-Rotor Transporting Unknown Varying Payload [J]. IEEE Access, 2020, 8(44671-86.

Zhang J, Li Y, Fei W, et al. Neural Network-Based Nonlinear Fixed-Time Adaptive Practical Tracking Control for Quadrotor Unmanned Aerial Vehicles [J]. Complexity, 2020, 2020(

Alqaisi W, Kali Y, Lucia W. Finite-Time Flight Control of Uncertain Quadrotor UAV based on Modified Non-Singular Fast Terminal Super-Twisting Control; proceedings of the 2020 IEEE Conference on Control Technology and Applications (CCTA), F 24-26 Aug. 2020, 2020 [C].

Song Y, He L, Zhang D, et al. Neuroadaptive Fault-Tolerant Control of Quadrotor UAVs: A More Affordable Solution [J]. 2019, 30(7): 1975-83.

Chen M, Wang H, Liu X. Adaptive Fuzzy Practical Fixed-Time Tracking Control of Nonlinear Systems [J]. IEEE Transactions on Fuzzy Systems, 2019, 1-.

Jiang B, Hu Q, Friswell M I. Fixed-Time Attitude Control for Rigid Spacecraft With Actuator Saturation and Faults [J]. IEEE Transactions on Control Systems Technology, 2016, 24(5): 1892-8.

Zhang J, Li Y, Fei W, et al. U-Model Based Adaptive Neural Networks Fixed-Time Backstepping Control for Uncertain Nonlinear System [J]. Mathematical Problems in Engineering, 2020, 2020(8302627.

Zhang J, Zhu Q, Li Y, et al. Homeomorphism Mapping Based Neural Networks for Finite Time Constraint Control of a Class of Nonaffine Pure-Feedback Nonlinear Systems [J]. Complexity, 2019, 2019

Xiao B, Yin S, Kaynak O. Attitude Stabilization Control of Flexible Satellites With High Accuracy: An Estimator-Based Approach [J]. IEEE/ASME Transactions on Mechatronics, 2017, 22(1): 349-58.

Liu W, Zhang J, Li B, et al. Finite-time Formation Tracking Control for Quadrotor UAVs Based on Fast Non-singular Terminal Sliding Mode; proceedings of the 2018 International Symposium in Sensing and Instrumentation in IoT Era (ISSI), F 6-7 Sept. 2018, 2018 [C].

Zhang J, Li Y, Fei W, et al. U-Model Based Adaptive Neural Networks Fixed-Time Backstepping Control for Uncertain Nonlinear System [J]. Mathematical Problems in Engineering, 2020, 2020

Chen F, Jiang R, Zhang K, et al. Robust Backstepping Sliding-Mode Control and Observer-Based Fault Estimation for a Quadrotor UAV [J]. IEEE Transactions on Industrial Electronics, 2016, 63(8): 5044-56.

Wenbo Fei is currently studying for a master's degree in the School of Electrical Engineering, Hebei University of Science and Technology, Hebei Province, China. His main research interests are neural network control of nonlinear systems and sliding mode control.

Jin Tian is currently studying for a master's degree in the School of Electrical Engineering, Hebei University of Science and Technology, Hebei Province, China. Her main research interests are Micro grid Control and Power Quality Improvement Technology

Xueli Wu was born in July 1961, Manchu, Qiqihar, Heilongjiang Province. In October 2005, he graduated from Huazhong University of Science and Technology. He joined the NLD in 1993. Since November 1998, he has been a professor and doctoral tutor at Hebei University of Science and Technology. He is currently the dean of the Science and Technology Development Research Institute of Hebei University of Science and Technology. In 2019, he was awarded as an excellent expert in provincial management in Hebei Province.